J. Chem. Lett. 4 (2023) 190-199

Research Article

Journal of Chemistry Letters
journal homepage: www.jchemlett.com
ISSN (online) 2717-1892 (print) 2821-0123

Phyto assisted Synthesis and Comparative Studies of Zinc Oxide Nanoparticles with *Ficus benghalensis* from Conventional Heating and Microwave Heating Method

Sonam Dawar[1, 2]*, Darshana Mehta[1] and B. K. Mehta[1]

[1]*School of Studies in Chemistry and Biochemistry, Vikram University, Ujjain, India*
[2] *Rani Durgawati Government Post Graduate College Mandla, India*

ARTICLE INFO

Article history:
Received 3 September 2023
Received in revised form 19 December 2023
Accepted 19 December 2023
Available online 19 December 2023

Keywords:
Ficusbenghalensis
Zinc Oxide nanoparticles
Microwave Heating
X-ray Diffraction
Dynamic Light Scattering
Antibacterial activity

ABSTRACT

This paper emphasizes on the comparative studies of Ficus (*Ficusbenghalensis*) bounded zinc oxide nanoparticles using conventional and microwave heating methods. Zinc oxide can be called a versatile material due to its unique physical and chemical properties. The resultant synthesized nanoparticle prepared using the conventional heating method and microwave heating method was termed as A-ZnO and B-ZnO nanoparticles respectively. The current study investigates the possible utilization of aerial roots of Ficus for the preparation of ZnO nanoparticles using zinc chloride as source material and sodium hydroxide as precipitant which involves a self-sustained reaction in a homogeneous solution. The resultant nanoparticles were characterized using UV-visible spectroscopy, Fourier Transform Infrared spectroscopy, X-ray diffraction, Dynamic Light Scattering, Zeta potential, Scanning Electron Microscopy with Energy Dispersive, X-Ray analysis and Transmission Electron Microscopy. ZnO nanoparticles prepared from both methods using conventional and microwave-assisted heating were compared. The prepared nanoparticles were characterized for their surface morphology. Further, the antibacterial activity of the extract and both ZnO NPs were evaluated against the standard and clinical strain of Gram-positive and Gram-negative bacteria by the agar well diffusion method. The results unveiled that the prepared ZnO NPs shows excellent antibacterial activity against the examined microorganisms. The overall study suggests that the root extract of the Ficus plant could work as an excellent bio-resource for producing ZnO NPs.

1. Introduction

In the last few decades, the Nanotechnology field has dealt with synthesis of leading, and fabricating nanomaterials, nanostructures, and nano devices with micromillimeter preciseness [1]. Size is amongst significant properties of nanoparticles. Its size within range of 10-100 nm is regarded ideal for biological and medical applications [2]. It is apparent that Nanomedicine is an area of biomedical application of nanotechnology within which synthesized and devised nanoparticles are utilized to treat illness [3]. ZnO nanoparticles show comparatively high biocompatibilityproperty which is ascribed due to semiconductor nature[4-5]. In the previous couple of years zinc oxide has upgraded itself as an engaging metal oxide material as a result of its distinctive properties like elevated chemical and mechanical stability, a varied range of radiation absorption, high catalysis activity, electrochemical coupling coefficient, nontoxic nature etc. [6]. The employment and big impact of nanomaterials in medical science is gaining plenteously response across the planet. The analysis focuses on the employment of varied nanostructured materials in several areas, like for drug delivery [7] and cancer treatments [8, 9].

FicusbenghalensisLinn.Syn. genus Ficus banyana Lorenz Oken. (Family Moraceae) is a giant evergreen tree found everywhere in India from the sub-Himalayan region to the deciduous forest south India. *F. benghalensis* tree plays a lead role in native structure of drugs like Ayurveda, Siddha, Unani and Homeopathy.

Aerial roots of *F. benghalensis* possess several properties like memory-boosting, antianxiety drug,

Corresponding author.; e-mail: sonamdawar03@gmail.com
https://doi.org/ 10.22034/jchemlett.2023.390724.1136

muscle relaxant, and seizure-modifying results [10]. They are usually utilized to cure styptic, syphilis, biliousness, infectious disease and inflammation of the liver. The aerial roots possess several flavonoids, terpenoids and steroids like bengalensinone, benganoic acid, lupanyl acetate, 3-acetoxy-9(11), 12-ursandiene, stigmasterol, 4-hydroxyacetophenone, 4-hydroxybenzoic acid, 4-hydroxymellein and *p*-coumeric acid [11, 12].

Green synthesis approaches are attracting a lot of attention due to comparatively lower costs and lesser practice of using poisonous chemicals and severe conditions for reduction and stabilization of nanoparticles [13]. Nanoparticles are environmentally friendly, supply fabrication and are less toxic, environmentally friendly and biocompatible which is why they are used in biological applications [14, 15]. Varied chemical ways are projected for the synthesis of ZnO NPs, like sol-gel combustion, chemical vapor deposition, sonochemical, micro-emulsion, freeze-drying and optical device ablation, hydrothermal synthesis, precipitation technique etc. These techniques, however, suffer varied disadvantages as a result of the involvement of high temperature and pressure conditions and toxic chemicals [16]. The green synthetic method involving biological plant extracts is an extensively acclaimed process owing to its merits, like it needs no extra chemicals, is simple, eco-friendly, cheap, and is a single step synthesis technique [17-20].

We have, in the present study reported the comparative studies of ZnO nanoparticles synthesis by conventional and microwave heating method utilizing *F. benghalensis* root extract as an efficacious reducing agent. The prepared ZnO NPs is tested for their morphological, structural and antimicrobial activity.

2. Experimental details

2.1. Preparation of extract

The aerial roots of *F. benghalensis* were collected. The material was cleaned thoroughly with tap water to eradicate any type of contamination. Washed aerial roots were air-dried in shade for 3 months. The aerial roots were powdered in a grinder and 250 g of powder and ethanol were filled in the soxhlet apparatus. The ethanolic extract was processed at 80-90 ^{o}C for 72 hours. The extract was concentrated under reduced pressure at a low temperature (40-50 ^{o}C).

2.2. Synthesis of nanoparticles

Before synthesis of ZnO NPs, the plant extract was thoroughly filtered by Whatman filter paper. Zinc chloride solution (25 %) was prepared in 100 mL deionized water. 5 mL of the above extract was slowly added with stirring in the 50 mL of 25% $ZnCl_2$ solution and stirred for 1 h in the magnetic stirrer. After 1.5 h, 50 mL 25% NaOH solution was added slowly into the solution containing $ZnCl_2$ and plant extract. The white precipitate formed was allowed to settle for 48 h. White precipitate of ZnO nanoparticles were separated by high-speed centrifugation. The supernatant clear solution was drained and the remaining precipitate was cleaned with distilled water several times. Finally, the precipitate was filtered using the suction pump and dried in a hot air oven at150 ^{O}C for 4 h. This sample is designated as A-ZnO NPs.

In another 250 mL conical flask, 5 mL of the above extract was slowly added with stirring in the 50 mL of 25% $ZnCl_2$ solution and stirred for 1 h in the magnetic stirrer. After 10 min, the conical flask was heated for 2 min with 800 W output into a microwave oven. After 2 min, the conical flask was taken out from the microwave oven and stirred for 30 sec and kept in the microwave oven for 1 min with 800 W output. Finally, the irradiated solution was filtered using a Whatman filter paper and 25 % of NaOH solution was added slowly and the white precipitate formed was allowed to settle for 48 h. The further process was followed as that of A-ZnO NPs and designated as B-ZnO NPs.

3. Characterization of ZnO nanoparticles

3.1. UV-Vis Spectroscopy

For UV-Visible spectroscopy, the resultant ZnO nanoparticles of the reactions were resuspended in equal amounts of sterile deionized water and spectrum scans were performed using Perkin Elmer Lambda 25 UV-Visible spectrophotometer in the school of studies in chemistry and biochemistry Ujjain, in the wavelength range of 200-700 nm.

3.2.Fourier Transform Infrared Spectroscopy

FT-IR spectroscopy helps establish the identity of various phytochemical constituents used in the mitigation and stabilization of the nanoparticles. FT-IR spectrum of dried and powdered ZnO nanoparticles was attained using Perkin Elmer FTIR SP 10 STD from the school of studies in chemistry, DAVV, Indore, in the scale of 4000-400 cm^{-1}.

3.3.X-Ray Diffraction

Completely dried samples of ZnO nanoparticles were taken for XRD analysis using Bruker D8 Advance X-ray diffractometer using condition like CuKα radiation (λ = 1.5406 Å), 40 kV- 40mA, 2θ/θ scanning mode. Data was analysed for the 2θ range of 10 to 90 degrees with a step of 0.0202 degrees.

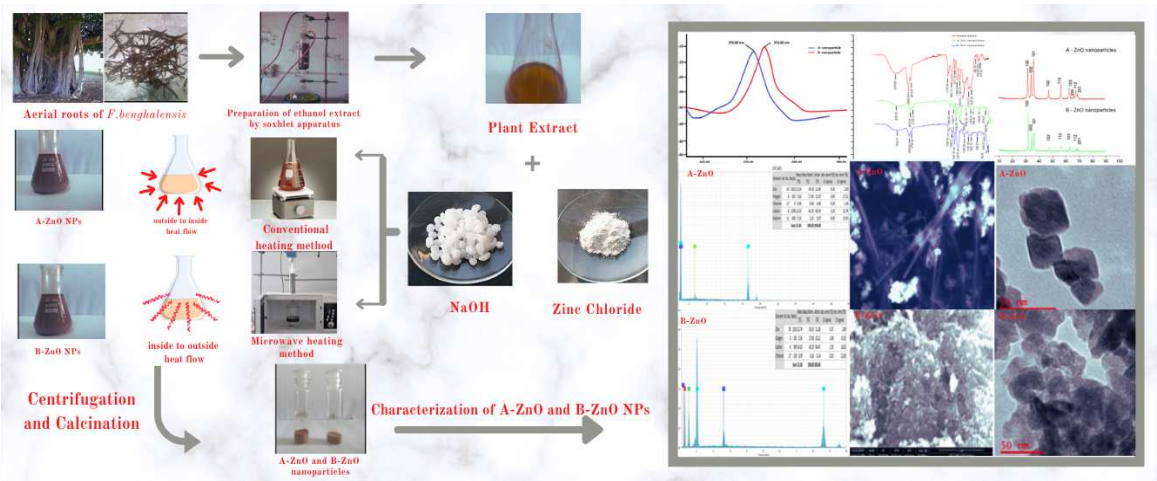

Scheme 1. The schematic representation of the preparation and characterization of both type of ZnO nanoparticals.

3.4. Field Emission Scanning Electron Microscopy and EDX

The morphology of the developed nanoparticles was examined using "FEI NoVANanoSEM 450" FESEM instrument operated at 18KV. The Energy Dispersive X-ray diffractive study was executed for both synthesized ZnO nanoparticles to determine elemental composition. Compositional analysis was made using "Bruker" made X-Flash 6130 EDX attachment and "Esprit" software.

3.5.Dynamic Light Scattering and Zeta Potential

DLS is an intensely and regularly used technique for hydrodynamic size distribution study. Using a zeta particle size analyzer NanoPlus-3 system, the hydrodynamic sizes and surface charges of bothsynthesized ZnO NPs were measured in deionized water as the suspension medium at pH 7

3.6.Transmission Electron Microscopy

The final shape of nanoparticles was studied by using TEM analysis. The ZnO NPs were mixed in sterile deionized water, sonicated for 20 minutesand diluted to produce a moderately turbid suspension. The suspension was then coated onto a copper grid and allowed to dry. TEM analysis of ZnO NPs was obtained using JEOL 1230 TEM fitted with a GATAN ORIUS CCD camera.

3.7. Antibacterial Activity Study

The antibacterial activity of extract and both ZnO NPs were evaluated against the standard and clinical strain of Gram-positive and Gram-negative bacteria (standard strains: *E. coli MTCC-1563, S. aureus MTCC-3160, P. aeruginosa MTCC-4643, K. pneumoniae MTCC-3040 and S. typhi MTCC-1253*) by the agar well diffusion method. For the wet heat sterilization of culture medium and glassware, they were keptin an autoclave at 15 psi for 15-20 minutes at 121°C and then glassware was heated in a hot air oven at 160°C for about 2 h. One litter of nutrient broth (HiMedia- GRM666-500G) was prepared by dissolving 13 g of commercially available nutrient broth in 1000mL distilled water and further agar-agar 1 (Lot GRM666) (20gm/1000ml) was added and boiled to dissolve the medium completely. The medium was sterilized by autoclaving at 15 lbs pressure (121ºC) for 15 minutes (Autoclave Model no: IS-4159). Petri plates containing 20mLnutrient agar medium were seeded with 24h culture of bacterial strains. On the reaction glass plate, wells were cut in which 20µL of the given sample (of different concentrations) were poured. The antibacterial activity was assayed by measuring the diameter of the inhibition zone formed around the well after incubation time for 24 hours at 37°C. Gentamicin, Ofloxacin and Azithromycin were used as the control. Antibacterial activity was evaluated by measuring the inhibition zone against the test microorganisms.

4. Result and discussion

4.1. UV-Visible Spectroscopy

The visual color change from half-white to grey-yellow is the preliminary visual indication of the transformation of the synthesis of ZnO NPs using freshly prepared extract. The absorption spectrum of both nanoparticles was recorded in the region 300-800 nm. For observation of spectrum, both nanoparticles powder was suspended in deionized water and placed in the cuvette. The UV-Visible spectra of A-ZnO NPs peak obtained at 370 nm and B-ZnO nanoparticles peak obtained at 374 nm demonstrate the existence of absorption characteristics of both ZnO nanoparticles as shown in Fig.1.This data is crucial for understanding the optical properties of the synthesized ZnO nanoparticles and can be used to correlate their size, structure, and electronic properties.

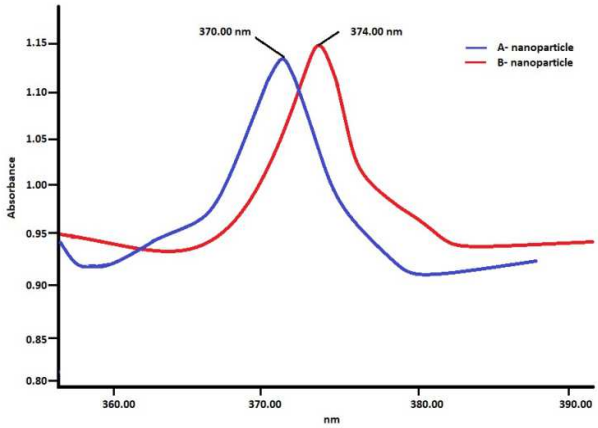

Fig. 1. UV-Vis spectra of A- ZnONPs and B- ZnONPs.

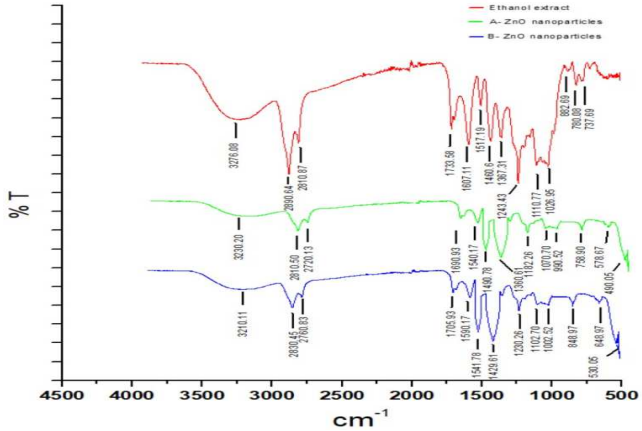

Fig. 2. Fourier transforms infrared spectra of *F. benghalensis* root extract, A-ZnONPs and B-ZnONPs.

4.2. FTIR analysis

Fourier Transform Infrared spectroscopy of the extract powder of *F. benghalensis* and synthesized A-ZnO and B-ZnONPsasillustrated in Fig.2 which reveals the possible secondary metabolites present in the ethanol extract which is responsible for the mitigation of zinc ions and mechanism of ZnONPs formation. The FTIR spectra of ethanol extract showed the broad band's due to −OH stretching frequency around 3444-3200 cm^{-1}[21].However, peaks at 2990 cm^{-1} and 2810 cm^{-1} are attributed to the asymmetric and symmetric stretching vibrations of the $-CH_2$ group respectively [22].Fig. 2 indicates the peak shifts after the reaction of $ZnCl_2$ solution with root extract. The 1730 cm^{-1} peak, results from C=O stretching from unsaturated aldehyde and ketone. The IR spectrum of Ethanol extract exhibits a band at 1612 cm^{-1} corresponding to the C=O (amide)[23], C=C stretching and NH_3^+ asymmetric bending mode.Peak in the scale of 1541 and 1429 cm^{-1} corresponded to C=C stretch in the aromatic ring and C=O stretch in polyphenols and C-N stretch of amide-I in protein [24]. Bands at 1289-1215 cm^{-1} correspond to C–N, C–O stretching and O-H bending vibration. Medium intensity band at 1185-1121 cm^{-1} is assigned to C–O–C linkage vibrations due to the existence of carboxylic acid and acid anhydrides like functional groups. The absorption peak at 1029 cm^{-1}represents the stretching vibration of C–O group of primary and secondary alcohols (C–O), while smaller peaks at 900–700 cm^{-1} were assigned to the aromatic bending vibration of C–H. Quite small peak obtained at 648.97 and 578.67 cm^{-1} corresponded to the existence of C-alkyl chloride and hexagonal phase ZnO [25].In addition to the absorption bands of the biomolecules used as reduction and stabilization (capping agents), a sharp band at 490 cm^{-1} is observed which is characteristic of Zn-O stretching vibration of ZnO [26].

4.3. X-ray diffractometry

From the X-ray diffraction data one can reveal the crystallinity and purity of the synthesized nanostructures. XRD patterns are the consequences ofdifferent crystallographic planes of the structure by the X-ray diffraction [27].The XRD data and analysis of A-ZnO and B-ZnO NPs are given in Table 1 and 2 respectively. The diffractogram as shown in Fig. 3 has been compared with the standard powder diffraction card of JCPDS file No. 00-036-1451. A-ZnO NPs X-ray diffraction peaks obtained at 2θ values of 31.73, 34.31, 36.23, 47.52, 56.56, 62.85 and 67.95 corresponded to the lattice plane (hkl) value(1 0 0), (0 0 2), (1 0 1), (1 0 2), (1 1 0), (1 0 3) and (1 1 2) orientation respectively. B-ZnONPs X-ray diffraction peak obtained at 2θ values of 31.75, 34.49, 36.26, 47.59, 56.57, 62.89 and 67.97degree in the experimental diffractogram have been identified to be due to zinc metal and corresponding to lattice plane (hkl) values (1 0 0), (0 0 2), (1 0 1), (1 0 2), (1 1 0), (1 0 3), (1 1 2) planes of zinc and are labelled in Fig.3. The details of these peaks are given in Table 1and 2. The XRD study has thus confirmed that the resultant particles in both the prepared samples were ZnO NPs having hexagonal structure.

The average crystalline size D of both A-ZnO and B-ZnONPs have been characterised from the observes diffractograms using the Debye-Scherrer formula,

$$D = \frac{0.9\lambda}{\beta \cos\theta} \quad \ldots (1)$$

Where 'λ'; wavelength of the X-rays used for diffraction and 'β'; full width at half maximum (FWHM) of a peak [28].To estimate FWHM, each of the peaks was fitted with a Gaussian function [29].The average size of both synthesized nanoparticle A-ZnO and B-ZnO NPs were found to be 20.41 nm and 25.69 nm respectively. The measurement of interplanar spacing between the atoms, d, has been calculated using Bragg's Law,

$$2d \sin\theta = n\lambda \quad \text{... (2)}$$

Where'n'; the order of diffraction pattern. In the present case n is equal to 1.

$$a = d\sqrt{h^2 + k^2 + l^2} \quad \text{... (3)}$$

The values of 'd' and lattice constant 'a'ofboth A- ZnO and B- ZnONPs were obtained and are given in Tables 1 and 2 respectively [29]. The absence of impurity peaks in the XRD pattern of the synthesized zinc oxide (ZnO) nanoparticles is a positive indication of the single phase and high purity of the ZnO NPs.

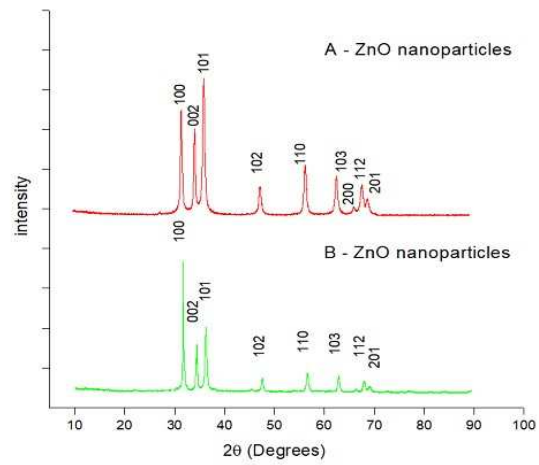

Fig. 3. X-ray diffraction pattern of the obtained A-ZnO NPs and B-ZnO NPs.

Table 1. Represents calculated interplanar distance and lattice constant of A-ZnO NPs.

S.No.	2 θ	θ	Cos θ	Sin θ	FWHM β degree	FWHM β radian	Size D	Inter-plannar spacing 'd'	hkl
1	31.73	15.86	0.96193	0.27328	0.38507	0.00671	21.48	2.81872	1 0 0
2	34.31	17.15	0.95553	0.29487	0.30011	0.00523	27.77	2.61233	0 0 2
3	36.23	18.11	0.95046	0.31084	0.42639	0.00743	19.63	2.47812	1 0 1
4	47.52	23.76	0.91524	0.40290	0.43458	0.00757	20.02	1.91188	1 0 2
5	56.56	28.28	0.88064	0.47378	0.49657	0.00866	18.18	1.62586	1 1 0
6	62.85	31.42	0.85336	0.52130	0.46653	0.00813	19.88	1.47705	1 0 3
7	67.95	33.97	0.82933	0.55875	0.60081	0.01047	15.96	1.37861	1 1 2

Table 2. Represents calculated interplanar distance and lattice constant of B-ZnO NPs.

S.No.	2 θ	θ	Cos θ	Sin θ	FWHM β degree	FWHM β radian	Size D	Inter-plannar spacing 'd'	hkl
1	31.75	15.87	0.96188	0.27345	0.21717	0.00378	38.18	2.81696	1 0 0
2	34.49	17.24	0.95507	0.29637	0.29934	0.00522	27.83	2.59911	0 0 2
3	36.26	18.13	0.95035	0.31117	0.36892	0.00643	22.68	2.47549	1 0 1
4	47.59	23.79	0.91503	0.40338	0.35102	0.00612	24.79	1.90961	1 0 2
5	56.57	28.28	0.88064	0.47378	0.40628	0.00708	22.24	1.62586	1 1 0
6	62.89	31.44	0.85318	0.52160	0.39425	0.00687	23.65	1.47680	1 0 3
7	67.97	33.98	0.82923	0.55890	0.46881	0.00817	20.47	1.37824	1 1 2

4.4. FESEM and EDAX

The effect of conventional and microwave-assisted synthesis on the final shape of both nanostructures was studied by using FESEM and EDAX analysis. SEM images were seen in different magnification ranges like 1µm- 10µm. A-ZnO NPs showed hexagonal tube-like structures and the B-ZnO NPs prepared by microwave heating method shows agglomeration of particles are in different shapes viz. spherical, trigonal and irregular in shape as shown in Fig. 4. The EDAX analysis confirmed the presence of metallic ZnO NPs. The composition obtained from EDAX analysis as shown in Fig.5. The EDAX analysis confirmed the presence and composition of ZnO nanoparticles. The EDAX spectrum A-ZnO NPs showed peaks of zinc and oxygen elements 39.38 and 17.65% proves ZnO nanoparticles prepared are essentially free from impurities. The EDAX pattern displayed of B-ZnO NPs shows that the developed products of the microwave heating method are made of zinc and oxygen of 39.10 and 17.06 %. The EDX analysis confirmed the presence of the required zinc (Zn) and oxygen (O) phases in the synthesized ZnO nanoparticles. The EDX graph revealing the existence of carbon (C), chlorine (Cl) and sodium (Na) also provides information about the elemental composition of nanoparticles and the surrounding environment. The presence of carbon in trace amounts indicates the involvement of plant phytochemical groups in the decrement and capping of the synthesized ZnO NPs [30]. We have developed a conventional and microwave heating route for zinc oxide nanoparticle synthesis. However the processing of zinc oxide nanoparticles utilizing *F. benghalensisisis* eco-friendly and can have positive implications for both the environment and potential applications of the nanoparticles, as eco-friendly synthesis methods are increasingly valued due to their reduced environmental impact.

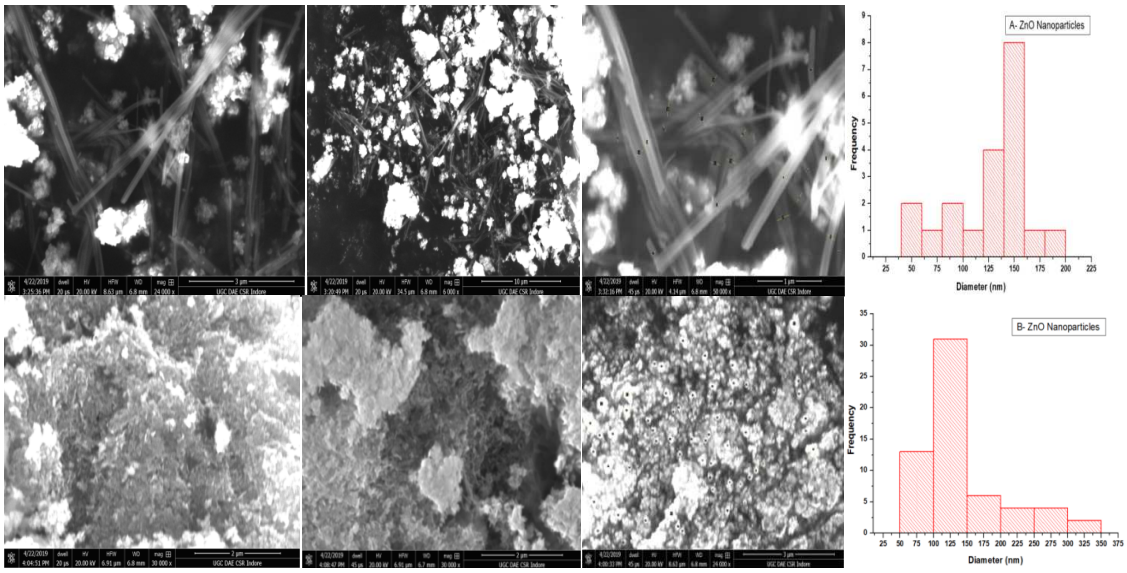

Fig. 4. Field Emission Scanning Electronic Microscopy (FESEM) images of A-ZnOand B-ZnONPs.

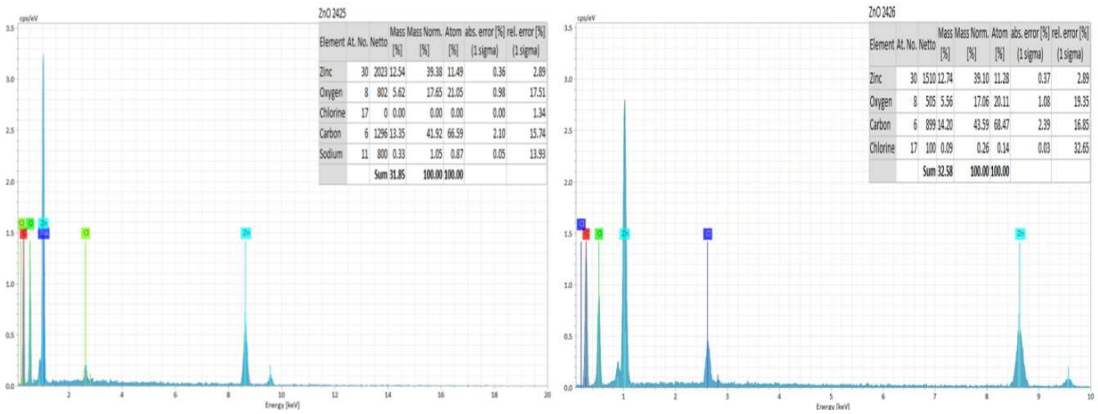

Fig. 5. Energy Dispersive Spectrum of A- ZnONPs and B- ZnONPs.

4.5. DLS and Zeta Potential

Dynamic light scattering (Photon Correlation Spectroscopy), is a powerful technique for probing particle sizes. The average size of particles, size distribution and polydispersity index of the synthesized both A-ZnO and B-ZnO NPs were determined by this technique. The A-ZnO and B-ZnO NPs average particle size was found to be 412.1 nm and 244.4nm respectively. The measured size of nanoparticles by DLS was moderately big size as compared to the SEM and TEM measurements since it determines the hydrodynamic radius of nanoparticles [30]. Polydispersity index was found 0.360 and 0.271 which indicates synthesized particles are monodispersed. The zeta potential of the both synthesized A-ZnO and B-ZnO NPs were determined in water as a dispersant. The zeta potential of the A- ZnO and B-ZnO colloidal solution was found to be -29.66mV and -23.19 mV respectively. The negative potential value showed by biosynthesized ZnO NPs could be due to the presence of bioorganic components in the extract as a capping agent. DLS and zeta potential distribution have been represented in Fig.6.

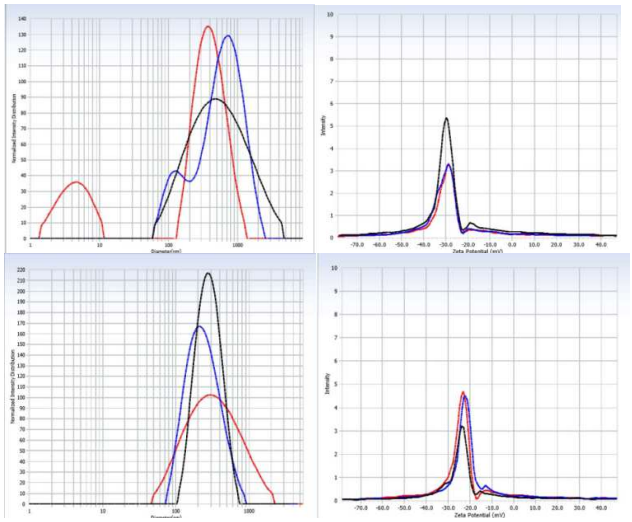

Fig. 6. DLS and Zeta Potential results of A- ZnONPs and B-ZnONPs.

4.6. TEM analysis

Transmission electron microscopy images give us information about the topography of the synthesized nanoparticles. TEM images of A-ZnONPs show a greater number of rod-like structures with a size range of 50-200 nm as shown in Fig.7and average nanoparticle size was 26.62 nm where as microwave-assisted ZnO nanoparticles revealed hexagonal structures with size range 50-100nm shown in Fig.7 and average nanoparticle size was 36.54 nm [31]. The microwave-assisted synthesis plays a major role in the preparation of ZnO nanoparticles using *F. benghalensis* aerial roots powder as a surfactant material which is confirmed by the TEM images. After analyzing the TEM images, we can find that the ZnO nanoparticles are concentrated at particular positions which show their tendency to aggregate [32].

4.7. Antibacterial activity

In vitro antibacterial activity of the aerial roots extract of *F. benghalensis* and synthesized A- ZnO and B-ZnONPs were determined using the agar well diffusion assay.The antibacterial activity of aerial roots extract of *F. benghalensis*, A-ZnO and B-ZnO NPs were evaluated by measuring the zone of inhibition against the test organisms [33]. The sizes of the zones of growth inhibition are presented in Table 3. The results indicate that the aerial roots extract of *F. benghalensis* and synthesized A-ZnO and B-ZnO NPs showed effective antibacterial activity against all tested strains. Arial roots of *F. benghalensis* extract and synthesized A-ZnO and B-ZnO NPs using were better against *P. aeruginosa* than gentamycin. In the case of *S. aureus*and*E. coli,*the sizes of the zones were approximately similar. In the case of *K. pneumoniae,* the size of the zone was less than floxacin and in the case of *S. typhi,*the size of the zone was approximately similar to compared with azithromycin [34].

During agar well diffusion assay, extract and nanomaterials accumulate in the wells of bacterial culture inoculated plate, where nanomaterials unleash and diffuse ions from the wells into the surrounding agar, it can interact with the bacteria, inhibiting their growth and form a zone of inhibition, often seen as a clear halo around the wells. When Both ZnO NPs encounter bacterial cells, they release zinc ions (Zn^{2+}) into the surrounding media which interfere with bacterial cell functions in several ways like disrupting of cell membrane and can also generate reactive oxygen species (ROS) such as free radicals when they come into contact with water and oxygen. ROS can cause oxidative stress within bacterial cells, damaging cellular components like DNA, proteins, and lipids. This oxidative stress contributes to cell damage and death. The combination of these mechanisms contributes to the antibacterial activity observed in the agar well diffusion assay (Fig.8).

Table 3. Zone inhibition of Extract and both ZnO NPs on different strains of microorganism

Microorganisms	Zones of growth inhibition (mm)					
	Extract	A-ZnO	B-ZnO	Gentamycin	Ofloxacin	Azithromycin
S. aureus MTCC-3160	12	16	19	21	-	-
E. coli MTCC-1563	16	17	18	21	-	-
P. aerugenosa MTCC-4643	20	21	22	19	-	-
K. pneumoniae MTCC-3040	10	13	17	-	20	-
S. typhi MTCC-1253	18	20	21	-	-	22

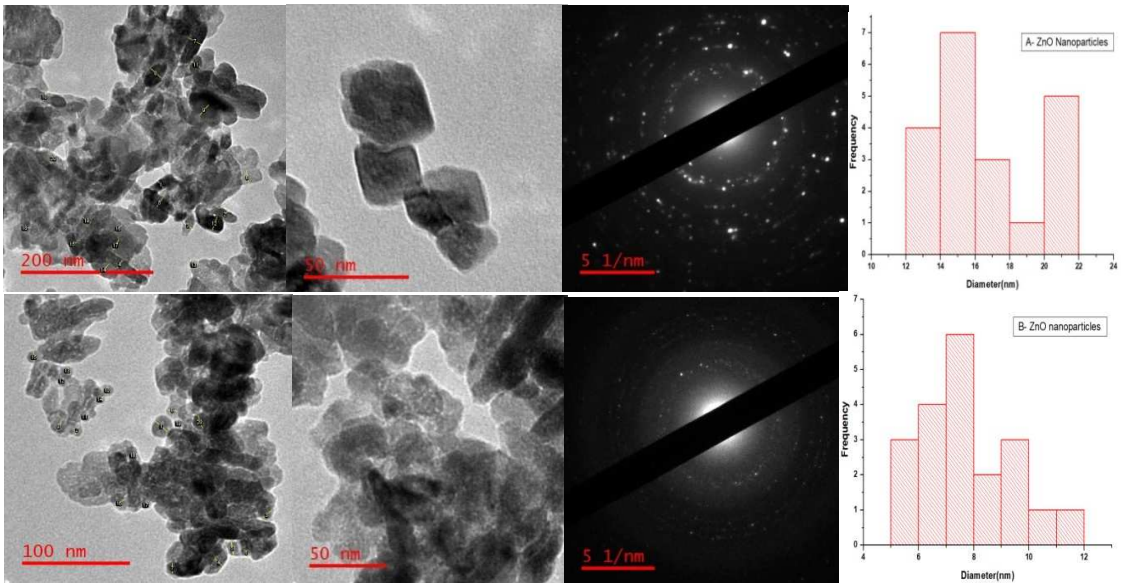

Fig. 7. Transmission Electronic Microscopy images of A- ZnOand B- ZnONPs.

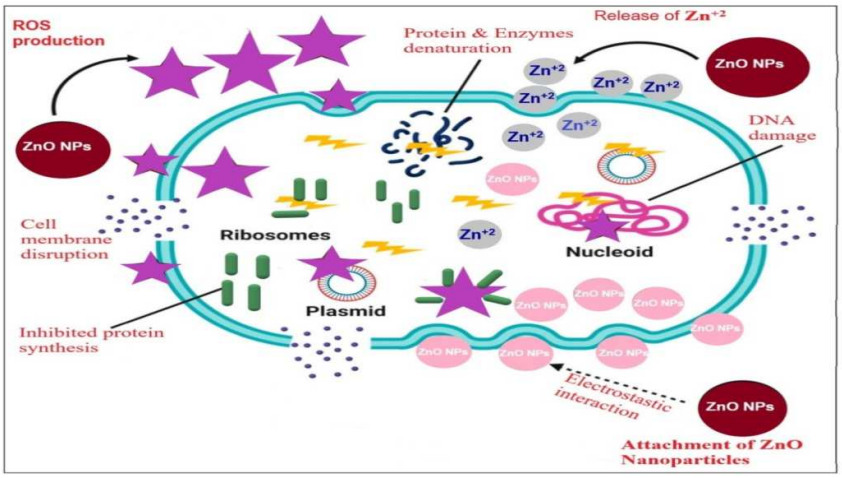

Fig. 8. The Schematic representation for the mechanism of antimicrobial activity.

5. Conclusion

The present study focuses on synthesizing zinc oxide (ZnO) nanoparticles using a cost-effective and environmentally friendly approach. The source of the nanoparticles is the ethanol extract obtained from the roots of *Ficus benghalensis*. Two heating methods, conventional heating and microwave heating, were compared for their effectiveness in synthesizing ZnO nanoparticles. Microwave heating was found to be superior to conventional heating in terms of reaction time, distribution of heating, and speed. This resulted in the formation of ZnO nanoparticles with specific structural characteristics.The UV-Visible spectroscopy measurements showed maximum absorbance in the range of 370-374 nm, indicating successful synthesis of A-ZnO and B-ZnO nanoparticles. Fourier Transform Infrared (FTIR) spectra were used to identify biomolecules and functional groups involved in ZnO nanoparticle synthesis and stabilization. Both ZnO nanoparticles synthesized using *F. benghalensis* roots had an average particle size of 20.41 nm (A-ZnO) and 25.69 nm (B-ZnO) as determined by XRD analysis.Scanning Electron Microscopy (SEM) analysis revealed tube-like structures in the nanoparticles, with larger particle sizes likely due to agglomeration of smaller particles. Energy Dispersive X-ray (EDX) analysis confirmed the presence of zinc oxide ions in the nanoparticles. A-ZnO nanoparticles had an average particle size of 412.1 nm, and B-ZnO nanoparticles had an average size of 244.4 nm. The polydispersity index indicated a relatively uniform size distribution. Zeta potential measurements were -29.66 mV for A-ZnO and -23.19 mV for B-ZnO, suggesting nanoparticle stability. The EDX analysis and elemental composition data support the involvement of plant phytochemicals in the nanoparticle synthesis process. For the nanoparticlesmorphology, Transmission Electron Microscopy (TEM) analysis displayed rod-like structures for A-ZnO nanoparticles and hexagonal-like structures for B-ZnO nanoparticles. Additionally, the study evaluated the antibacterial potential of the aerial root extract of *F. benghalensis*, A-ZnO nanoparticles, and B-ZnO nanoparticles against various bacterial strains. These nanoparticles showed antibacterial activity against *S. aureus, E. coli, P. aeruginosa, K. pneumoniae, and S. typhi*.The study overall establishes the potential of biogenically synthesized ZnO nanoparticles as antibacterial agents, particularly against multidrug-resistant bacteria. However, further investigation is required to fully understand the mechanisms underlying this antibacterial activity and to potentially develop these nanoparticles into effective therapeutic agents.

Acknowledgments

This research was supported by the Council of Scientific and Industrial Research (CSIR). The authors sincerely thank CSIR for providing the fellowship in terms of CSIR-SRF (File No. 09/176(0006)/2017-EMR-I). We would like to thank the Centre-director, Dr. V. Ganeshan, UGC-DAE, and Indore for allowing us to utilize available national facilities. We also thank to Dr. M. Gupta, Dr. G. Okram and Dr. D. M. Phase, UGC-DAE CSR, Indore for providing XRD, DLS and Zeta Potential and FESEM with EDAX facilities respectively. Central Instrumentation Facility, Gwalior is also gratefully acknowledged for providing the TEM data. We also thank Dr. S. Sharma, DAVV Indore for providing FTIR facility.

References

[1] G. Bisht, S. Rayamajhi, ZnO Nanoparticles: A Promising Anticancer Agent. *Nano Biomed.*, 3 (2016) 1-11.

[2] K. Huang, H. Ma, J. Liu, S. Huo, A. Kumar, T. Wei, Size-dependent localization and penetration of ultrasmall gold nanoparticles in cancer cells, multicellular spheroids, and tumors *in vivo*. *ACS Nano*., 6 (2012) 4483-4493.

[3] R. Wang, P.S. Billone, W.M. Mullett, Nanomedicine in Action: An Overview of Cancer Nanomedicine on the Market and in Clinical Trials. *J. Nanomater*., 2013 (2013) 1-12.

[4] J. Zhou, N.S. Xu, Z.L. Wang, Dissolving behavior and stability of ZnO wires in biofluids: a study on biodegradability and biocompatibility of ZnO nanostructures. *Adv. Mater.,* 18 (2006) 2432-2435.

[5] J.W. Rasmussen, E. Martinez, P. Louka, D.G. Wingett, Zinc oxide nanoparticles for selective destruction of tumor cells and potential for drug delivery applications. *Expert Opin Drug Deliv*., 7 (2010) 1063-77.

[6] C.M. Ananthu, B. Renjanadevi, Preparation of Zinc Oxide Nanoparticles and its characterization using Scanning Electron Microscopy (SEM) and X-Ray Diffraction (XRD). *Proc. Technol*., 24 (2016) 761-766.

[7] G.F. Paciotti, L. Myer, D. Weinreich, D. Goia, N. Pavel, R.E. McLaughlin, L. Tamarkin, Colloidal gold: a novel nanoparticle vector for tumor directed drug delivery. *Drug Deliv*., 11 (2004) 169-183.

[8] X. Wu, H. Liu, J. Liu, K.N. Haley, J.A. Treadway, J.P. Larson, N. Ge, F. Peale, M.P. Bruchez, Immunofluorescent labeling of cancer marker Her2 and other cellular targets with semiconductor quantum dots. *Nat. Biotechnol.,* 21 (2002) 41–46.

[9] L.R. Hirsch, R.J. Stafford, J.A. Bankson, S.R. Sershen, B. Rivera, R.E. Price, J.D. Hazle, N.J. Halas, J.L. West, Nanoshell-mediated near-infrared thermal therapy of tumors under magnetic resonance guidance. *Proc. Natl. Acad. Sci. U. S. A*., 100 (2003) 13549-13554.

[10] D.R. Panday, G.P. Rauniar, Effect of root-extracts of *Ficus benghalensis* (Banyan) in memory, anxiety, muscle co-ordination and seizure in animal models. *BMC Complement Altern Med.*, 16 (2016) 429.

[11] S.A. Fegade, M. Siddaiah, Isolation and Characterization of *Ficus* bengalensis Linn. *J. Drug Deliv. ther*., 9 (2019) 207-211.

[12] N. Riaz, M.A. Naveed, M. Saleem, B. Jabeen, M. Ashraf, S.A. Ejaz, Cholinesterase inhibitory constituents from Ficusbengalensis. *J. Asian Nat. Prod. Res.,* 14 (2012) 1149-1155.

[13] C. Mason, S. Vivekanandhan, M. Misra, A.K. Mohanty, Switchgrass (Panicumvirgatum) extract mediated green synthesis of silver nanoparticles. *World J. Nano Sci. Eng.,* 2 (2012) 47-52.

[14] M.S. Chavali, M.P. Nikolova, Metal oxide nanoparticles and their applications in nanotechnology. *SN Appl. Sci.,* 1 (2019) 607.

[15] N.L. Rosi, C.A. Mirkin, Nanostructures in biodiagnostics. Chem. *Rev.,* 105 (2005) 1547-1562.

[16] S. Sabir, M. Arshad, S.K. Chaudhari, Zinc oxide nanoparticles for revolutionizing agriculture: synthesis and applications. *Sci.World J*., 2014 (2014) 8.

[17] S.M. Pourmortazavi, Z. Marashianpour, M.S. Karimi, M. Mohammad-Zadeh, Electrochemical synthesis and characterization of zinc carbonate and zinc oxide nanoparticles. *J. Mol. Struct. Macromol.,* 1099 (2015) 232-238.

[18] S. Jafarirad, M. Mehrabi, B. Divband, M. Kosari-Nasab, Bio fabrication of zinc oxide nanoparticles using fruit extract of *Rosa canina* and their toxic potential against bacteria: a mechanistic approach. *Mater. Sci. Eng.*, 59 (2016) 296–302.

[19] T. Bhuyan, K. Mishra, M. Khanuja, A. Varma, Comparative study of pure and copper (Cu)-doped ZnO nanorods for antibacterial and photocatalytic applications with their mechanism of action. *J. Nanopart. Res.,* 17 (2015) 1-11.

[20] B. Bhuyan, B. Paul, D.D. Purkayastha, S.S. Dhar, S. Behera, Facile synthesis and characterization of zinc oxide nanoparticles and studies of their catalytic activity towards ultrasound-assisted degradation of metronidazole. *Mater.Lett.,* 168 (2016) 158–162.

[21] J.S. Kumar, S.V. Kumar, S.R. kumar, Synthesis of zinc oxide nanoparticles using plant leaf extract against urinary tract infection pathogen. *Res-eff Tech.,* 3 (2017) 459–465.

[22] A. Saidfar, A. Mohammad, P. Sajad, Application of Nano-sized poly (N-methyl pyrrole-pyrolle) Fiber to the Headspace Solid-Phase Microetraction of Volatile Organic Compounds from Yogurt. *J. Chem. Lett.*, 1 (2020) 39-46.

[23] P.O. Ameh, Synthesized iron oxide nanoparticles from *Acacia nilotica*leaves for the sequestration of some heavy metal ions in aqueous solutions. *J. Chem. Lett.*, 4 (2023) 1-13.

[24] M.A. Tijjani, Isolation and Structural analysis (Gas hromatography-Mass Spectrometry, Infra-red and Ultraviolet Spectroscopy) of leaf Ficus sycomorus Linn Moraceae. *J. Chem. Lett.*, 2 (2021) 33-42.

[25] S. Yedurkar, C. Maurya, P. Mahanwar, Biosynthesis of zinc oxide nanoparticles using *Ixoracoccinea* leaf extract—a green approach. *Open J. Synth. Theory Appl.,* 5 (2016) 1–14.

[26] T. Umasangari, S. Anandhavelu, S. Thambidurai, Eco-Friendly Preparation of Zinc Oxide Nanoparticles with Jackfruit Seed Flour Template and Microwave Assisted Heating. *Adv. Sci. Eng*., 5 (2013) 1-5.

[27] I. Martins, A. Hamza, O. Clifford, Effect of Filler Type o Crystallinity of Low-density Polyethylene Composites. *J. Chem. Lett.*, 1 (2020) 155-159.

[28] H.O. Hassani, S. Rakass, F.T. Al-wadaani, K.J. Al-ghamdi, A. Omer, M. Messali and M. Abboudi, Synthesis, characteriation and phytocatalytic activity of α-Bi_2O_3 nanoparticales. *J. Taibah Univ. sci*., 9 (2015) 508-512.

[29] B.K. Mehta, B.D. Shrivastava, M. Chhajlani, Green synthesis of silver nanoparticles and their characterization by XRD. *J. Phys. Conf. Ser*., 836 (2017) 1-4.

[30] T.I. Shaheen, M.E. El-Naggar, A.M. Abdelgawad, A. Hebeish, Durable antibacterial and UV protections of *in situ* synthesized zinc oxide nanoparticles onto cotton fabrics. *Int. J. Biol. Mac*., 83 (2016) 426-432.

[31] J.E. Jeronsia, L.A. Joseph, M.M. Jaculine, P.A. Vinosha and S.J. Das, Hydrothermal synthesis of zinc stannate nanoparticles for antibacterial applications. *J. Taibah Univ. sci*., 10 (2016) 601-606.

[32] P. Jamdagni, P. Khatri, J.S. Rana, Green synthesis of zinc oxide nanoparticles using flower extract of Nyctanthesarbortristis and their antifungal activity. *J. King Saud Univ. Sci.,* 30 (2018) 168-175.

[33] G. Sharma, R. Soni and N.D. Jasuja, Phytoassisted synthesis of magnesium oxide nanoparticles with *swertiachirayaita. J. Taibah Univ. sci*., 11 (2017) 471-477.

[34] O. Yamamoto, Influence of particle size on the antibacterial activity of zinc oxide. *Int. J. Inorg. Mater.*, 3 (2001) 643–646.